All silicon approach to modulation and detection at λ = 2 μm

Callum G. Littlejohns[*,a,b], Milos Nedeljkovic[b], Wei Cao[b], Jordi Soler Penades[b], David Hagan[c], Jason J. Ackert[c], Mohamed Saïd Rouifed[a], Wanjun Wang[a], Zecen Zhang[a], Haodong Qiu[a], Tina Guo Xin[a], Andrew P. Knights[c], Graham T. Reed[b], Goran Z. Mashanovich[b], Hong Wang[a], and David J. Thomson[b].

[a]Si Technologies Centre of Excellence, Nanyang Technological University, 639798, Singapore;
[b]Optoelectronics Research Centre, University of Southampton, Southampton, SO17 1BJ, UK;
[c]Department of Engineering Physics, McMaster University, Hamilton, Ontario, L8S 4L7, Canada.

ABSTRACT

Silicon photonics has traditionally focused on near infrared wavelengths, with tremendous progress seen over the past decade. However, more recently, research has extended into mid infrared wavelengths of 2 μm and beyond. Optical modulators are a key component for silicon photonics interconnects at both the conventional communication wavelengths of 1.3 μm and 1.55 μm, and the emerging mid-infrared wavelengths. The mid-infrared wavelength range is particularly interesting for a number of applications, including sensing, healthcare and communications. The absorption band of conventional germanium photodetectors only extends to approximately 1.55 μm, so alternative methods of photodetection are required for the mid-infrared wavelengths. One possible CMOS compatible solution is a silicon defect detector. Here, we present our recent results in these areas. Modulation at the wavelength of 2 μm has been theoretically investigated, and photodetection above 25 Gb/s has been practically demonstrated.

Keywords: silicon photonics, optical modulators, photodetectors, mid-infrared

1. INTRODUCTION

Silicon photonics has been extensively researched over the last several decades because it provides a route to the realisation of low cost photonic integrated circuits through fabrication that is synonymous with CMOS electronic fabrication i.e. high volume and high yield. The majority of research focusses on the near infrared (NIR) wavelengths of 1.33 μm and 1.55 μm. Key components of a silicon photonics interconnect are modulators and photodetectors, and tremendous progress has been made in the realisation of these high performance devices. Successful demonstrations have been made of modulators that are based upon the plasma dispersion effect[1], as well as hybrid approaches involving the incorporation of other materials such as III-V compounds[2], SiGe[3], graphene[4], or organic materials[5]. On the component level, a large amount of research is ongoing worldwide to achieve increased levels of performance in different metrics such as speed, power consumption, modulation depth, footprint, wavelength independence, temperature insensitivity, and optical loss. Photodetection has typically been achieved at NIR wavelengths in germanium[6-9], with high performance waveguide integrated devices now considered a mature process.

However, the mid-infrared (MIR) domain (2-20 μm) is becoming increasingly popular[10-15] due to many interesting applications in sensing, healthcare and communications.

The wavelength of 2 μm is of particular interest to the communications industry because of the ability to exploit the amplification capabilities of the direct diode-pumped monolithic thulium-doped fiber amplifier (TDFA)[16] and the low-loss and low latency potential of transmission systems based on hollow core photonic band gap fibers (HC-PBGF)[17]. HC-PBGFs, with a minimum loss observed around 2 μm, offer a radical solution to increase transmission capacity per fiber, decrease fiber loss and nonlinearity, and reduce signal latency when compared to the state-of-the-art in the traditional[18] communication bands.

*Corresponding author email address: clittlejohns@ntu.edu.sg

2. OPTICAL MODULATION AT 2 µm

The plasma dispersion effect is a well-known effect which relates changes in electron and hole concentrations to changes in refractive index, n, and optical absorption, α. It is the most commonly used modulation mechanism in silicon, due to the lack of a Pockels effect in the centro-symmetric silicon crystal. In 2011, Nedeljkovic et al.[19] published refined expressions linking refractive index and optical absorption to free carrier densities for wavelengths spanning from the NIR, to deep into the MIR. The expressions at λ = 1.55 µm are shown below:

$$(@\ \lambda = 1.55\ \mu m)\ -\Delta n = 5.40\times10^{-22}.\Delta N_e^{1.011} + 1.53\times10^{-18}.\Delta N_h^{0.838}$$
$$(@\ \lambda = 1.55\ \mu m)\ \Delta\alpha = 8.88\times10^{-22}.\Delta N_e^{1.167} + 5.84\times10^{-20}.\Delta N_h^{1.109}$$

Where ΔN_e and ΔN_h are the changes in free electron and hole concentrations, respectively. Additionally, the expressions at λ = 2 µm are:

$$(@\ \lambda = 2\ \mu m)\ -\Delta n = 1.91\times10^{-21}.\Delta N_e^{0.992} + 2.28\times10^{-18}.\Delta N_h^{0.841}$$
$$(@\ \lambda = 2\ \mu m)\ \Delta\alpha = 3.22\times10^{-20}.\Delta N_e^{1.149} + 6.21\times10^{-20}.\Delta N_h^{1.119}$$

It can be seen from these expressions that both the refractive index change and the absorption coefficient change are more efficient at λ = 2 µm when compared to λ = 1.55 µm. This is perhaps better depicted graphically, as shown in Figure 1:

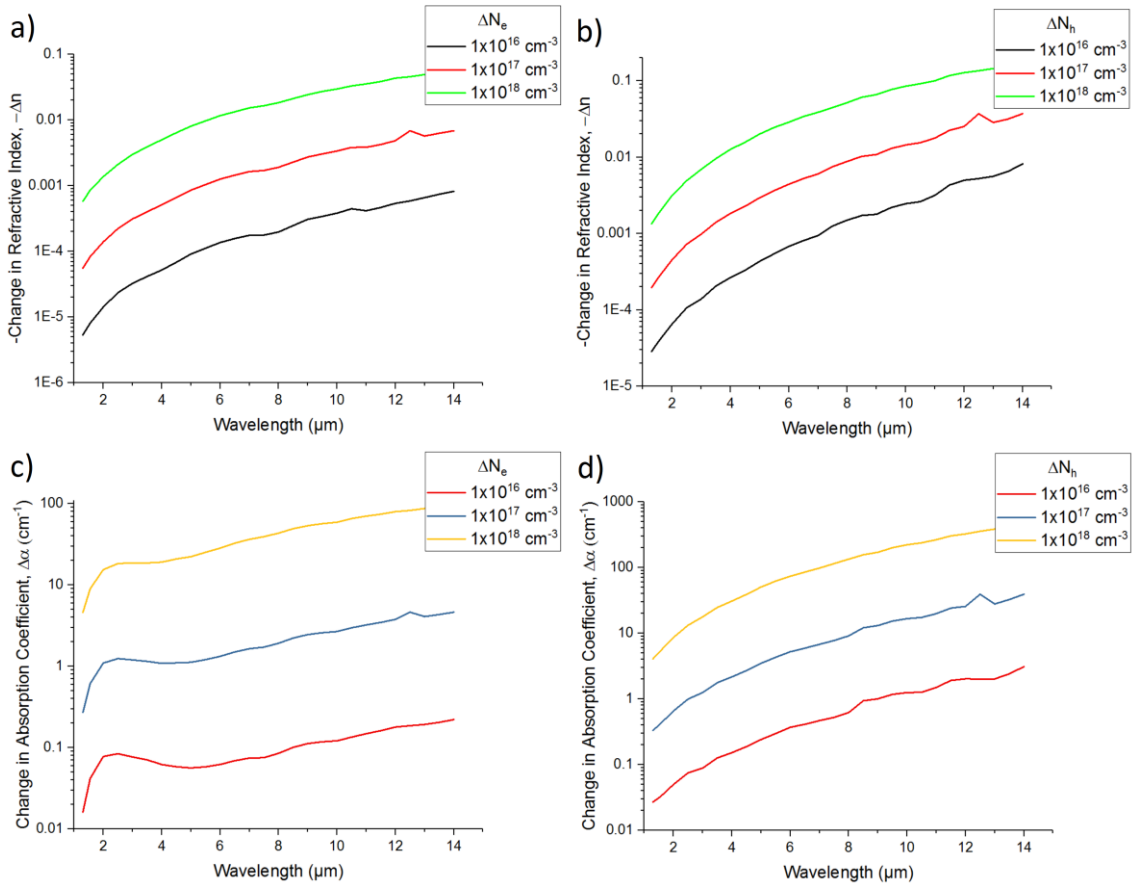

Figure 1. Plasma dispersion effect as a function of wavelength for a range of free carrier concentrations, using data from ref.[19], a) Change in electron concentration effect on refractive index, b) Change in hole concentration effect on refractive index, c) Change in electron concentration effect on absorption coefficient, d) Change in hole concentration effect on absorption coefficient.

It is evident from the graphs in Figure 1 that the desirable increase in refractive index change at $\lambda = 2$ µm is also accompanied with an undesirable (in the case of carrier depletion modulators) increase in absorption. It is also evident that the hole free carrier density has a stronger effect on both the refractive index and absorption coefficient than the electron free carrier density at $\lambda = 2$ µm.

Using the 220 nm silicon-on-insulator (SOI) platform, a Mach-Zehnder based carrier depletion modulator has been designed with the phase shifter cross section shown in Figure 2. The position of the p-n junction offset has been varied, as well as the high doping separation, with the simulated optical loss and L_π plotted in Figure 3.

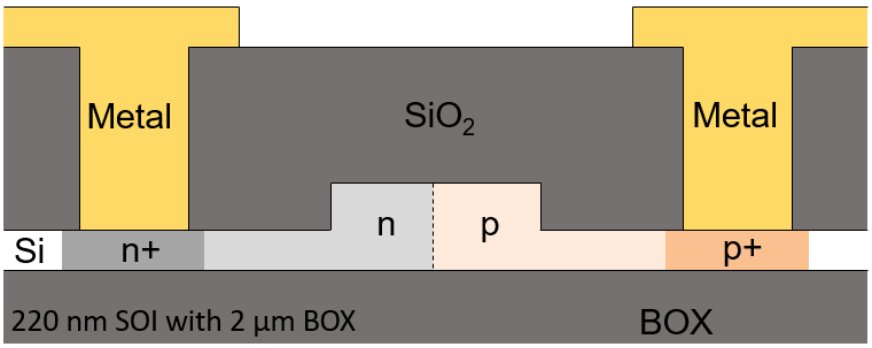

Figure 2. Cross-section schematic of $\lambda = 2$ µm carrier depletion modulator.

A combination of electrical simulations using Silvaco and optical simulations using a MATLAB based mode solver was used to analyse the phase shifter response. The free carrier distribution under zero bias and reverse bias was first simulated using the electrical device model built in Silvaco. This distribution is converted into a change in refractive index and absorption coefficient using the Nedeljkovic equations[19] and input into a MATLAB based mode solver considering both the free carrier effects, and the baseline material refractive index. The performance of the device is evaluated through the effective refractive index and loss of each optical mode.

From the graphs shown in Figure 3 it is evident that the high doping separation should be at least 1.2 µm in order to avoid introducing excessive optical loss due to optical mode leakage into the highly doped regions. The phase shifter length required in order to achieve a pi phase shift is reduced to approximately 4 mm under a reverse bias of 6 V, compared with a length of 17 mm under a reverse bias of 2 V. This is due to the increase in the depletion region width as the reverse bias increases, resulting in a greater change in refractive index.

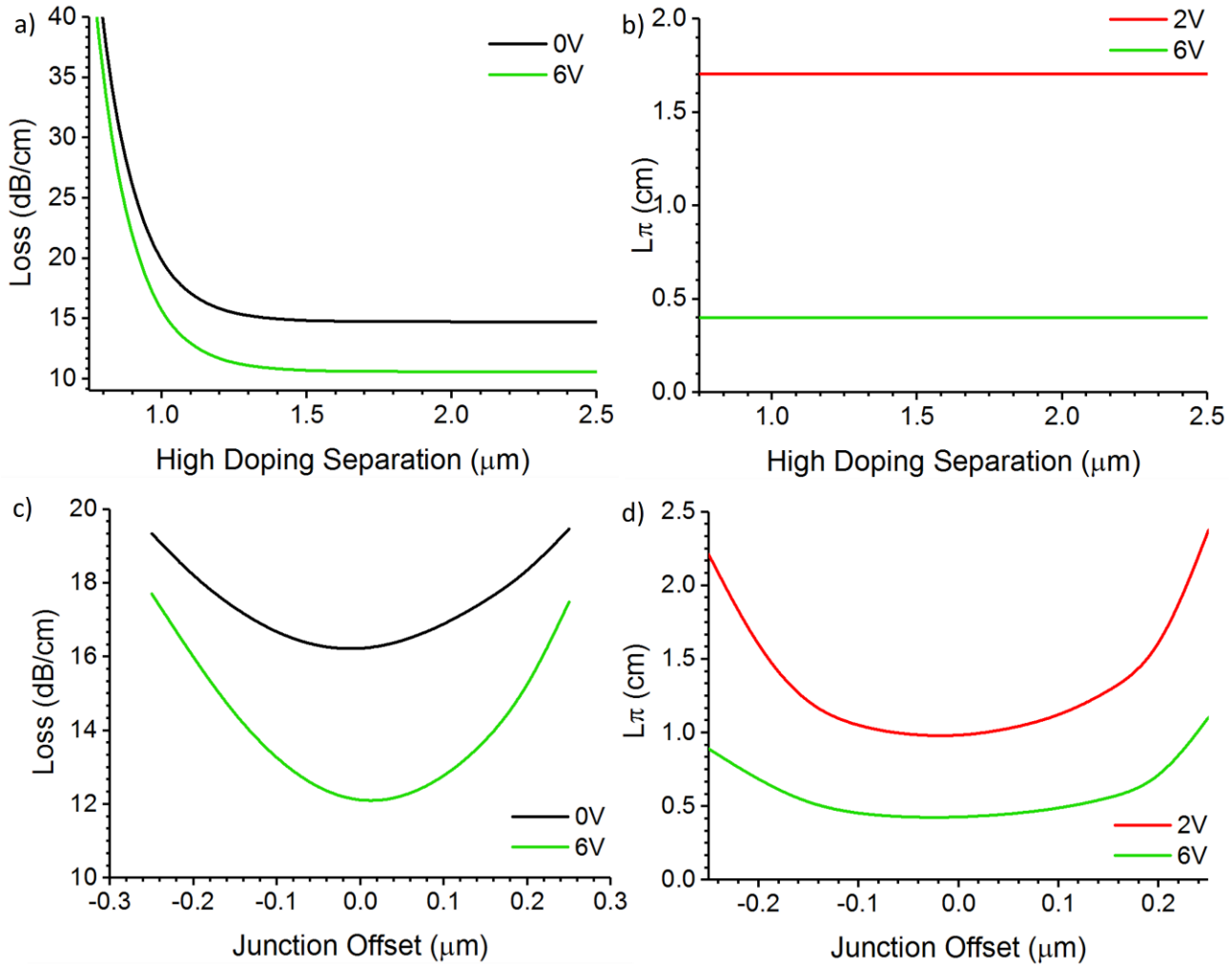

Figure 3. Simulated DC phase shifter performance of $\lambda = 1.95$ μm carrier depletion modulator at zero volts and various reverse biases, a) optical loss as a function of highly doped region separation, b) pi phase shift length as a function of highly doped region separation, c) optical loss as a function of p-n junction offset position relative to the centre of the waveguide, d) pi phase shift length as a function of p-n junction offset position relative to the centre of the waveguide.

3. OPTICAL DETECTION AT 2 μm

Optical detection at MIR wavelengths is complicated by the fact the germanium absorption band does not extend beyond approximately 1.6 μm. Therefore, alternative method of photodetection are required. A potential mechanism is defect induced trap-assisted absorption. Such defect detectors can be formed in silicon, and therefore avoid the complication of epitaxial growth of another material. Here, a defect detector is formed in the 220 nm SOI platform. First, waveguides are etched, and highly doped regions are subsequently formed by ion implantation in order to form a p-i-n junction across the waveguide. The highly doped regions can be formed simultaneously with the modulator highly doped regions if fully integrated circuits are desired. Next, a silicon dioxide cladding is added, vias etched and metal contacts formed. The only additional processing steps required from a typical modulator process is a final top cladding etch in order to open implantation windows, and a final ion implantation to introduce defects into the waveguide. A boron implant at an energy of 60 keV and a dose of $1x10^{13}.cm^{-2}$ is used here. The device cross section is shown in Figure 4. The device length is 1 mm, the waveguide width is 1 μm, and the doping separation is 1.6 μm.

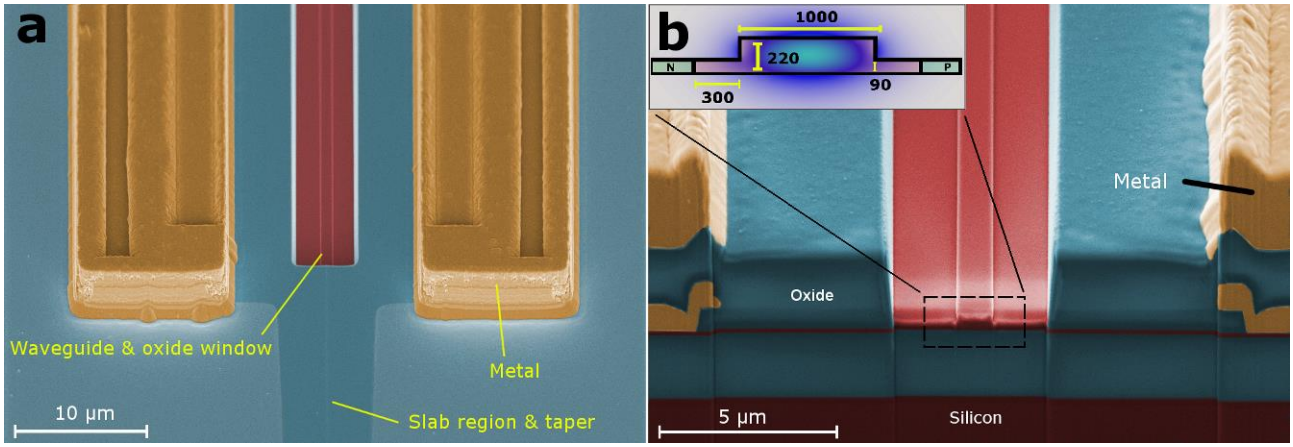

Figure 4. SEM images of λ = 2 µm defect detectors, a) Entire device showing implantation window into the waveguide, b) focused ion beam cross section of the device. Reprinted by permission from Springer Customer Service Centre GmbH from ref[20] [COPYRIGHT] (2015).

The characterisation setup is described in Figure 5. Light from a 2 µm tunable laser is amplified by a custom built thulium doped fibre amplifier (TDFA). A commercial 10 GHz lithium niobate modulator provides a modulated optical signal to the device. Coupling to the chip is achieved with the butt coupling method via a tapered fibre. The detector output signal is measured using a digital communication analyser (DCA).

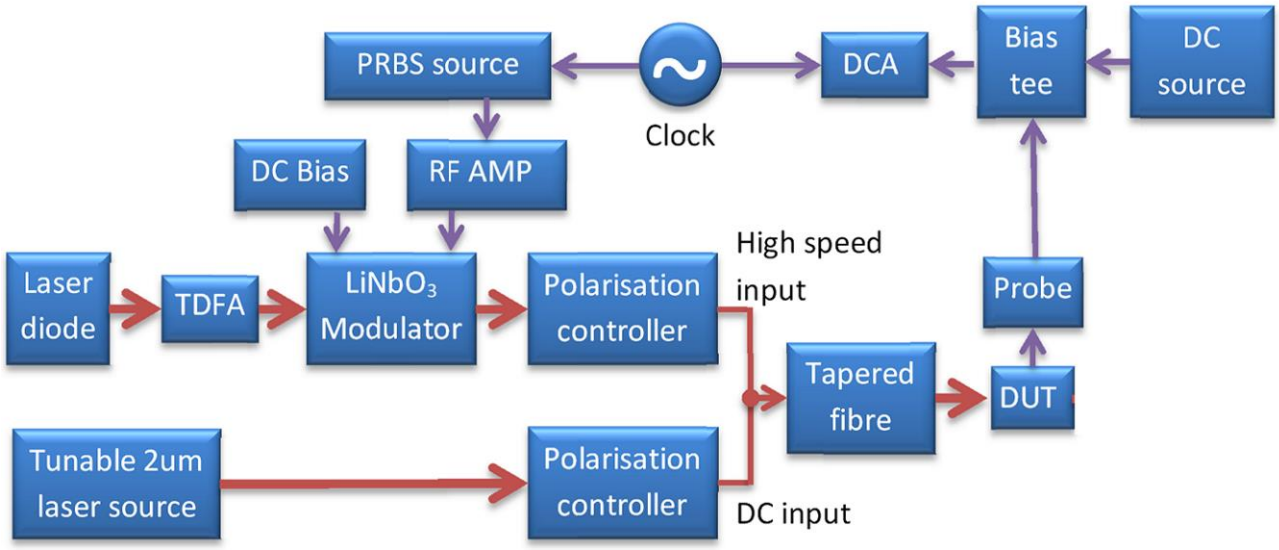

Figure 5. Characterisation setup for λ = 2 µm photodetectors.

The device is operated in avalanche mode in order to improve its responsivity, which is measured to be 0.3 ± 0.02 A/W at a reverse bias of 30 V. The dark current is less than 1 µA, even at this high reverse bias. Figure 6a shows the device DC performance under both dark and illuminated conditions at a wavelength of 2.02 µm as a function of reverse bias. Figure 6b shows the DC performance as a function of wavelength under both 10 V and 25 V reverse bias.

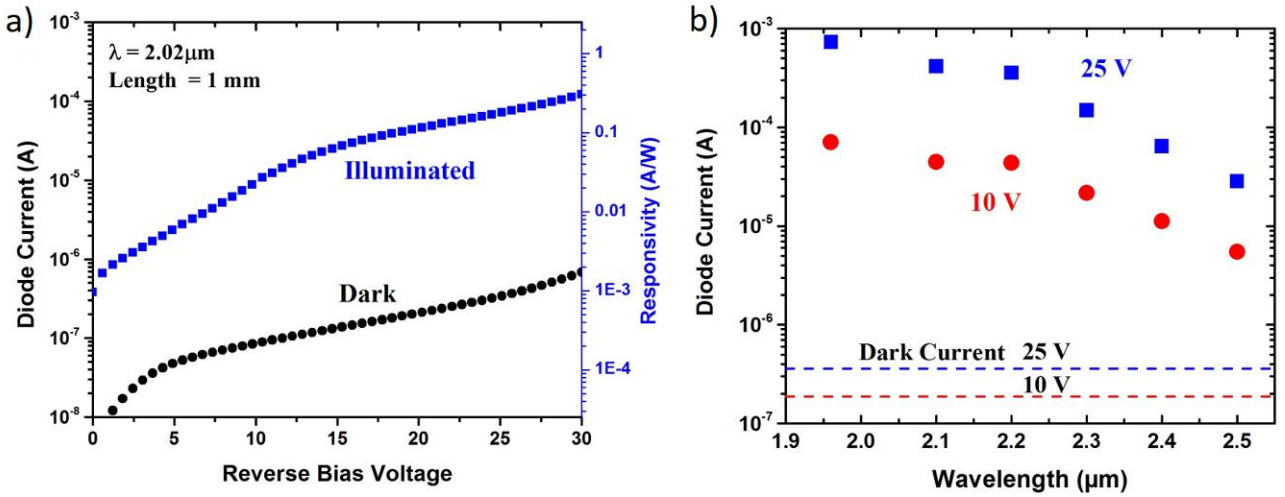

Figure 6. DC characteristics of λ = 2 μm defect detector, a) as a function of reverse bias, b) as a function of wavelength. Reprinted by permission from Springer Customer Service Centre GmbH from ref[20] [COPYRIGHT] (2015).

The device is also characterised at high speed. The eye diagrams are shown in Figure 7, showing high speed operation at 28 Gbit/s at a reverse bias of 27 V.

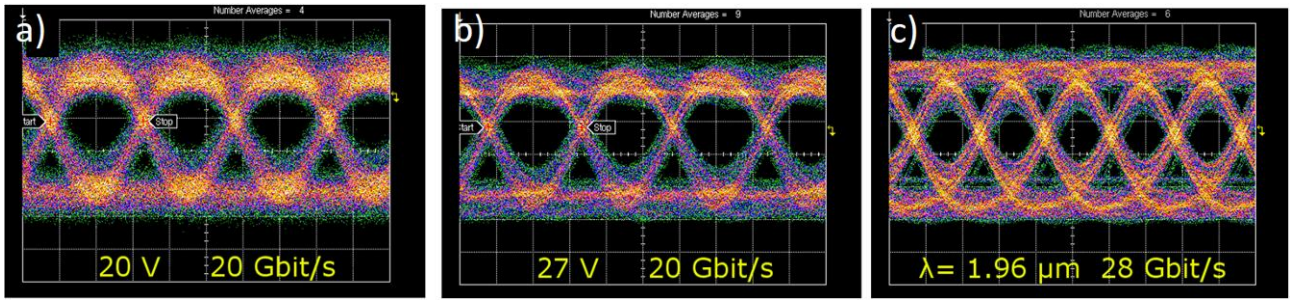

Figure 7. Eye diagrams of λ = 2 μm defect detector at a wavelength of λ = 1.96 μm, a) 20 Gbit/s at 20 V reverse bias, b) 20 Gbit/s at 27 V reverse bias, and c) 28 Gbit/s at 27 V reverse bias. The vertical scale is 6.7 mV per division. Reprinted by permission from Springer Customer Service Centre GmbH from ref[20] [COPYRIGHT] (2015).

4. CONCLUSION

An all silicon approach has been taken to optical modulation and photodetection at the MIR wavelength of 2 μm. This approach avoids the complexity of introducing new materials to the SOI platform and therefore greatly simplifies fabrication of devices at this wavelength, consequently also reducing cost. The wavelength of 2 μm is of particular interest because of the potential of both the TDFA and low loss HC-PBF's.

ACKNOWLEDGEMENTS

The research leading to these results was funded by the UK Engineering and Physical Sciences Research Council (EPSRC) under the grants "Silicon Photonics for Future Systems" and "MIGRATION", and is also supported by the National Research Foundation of Singapore (NRF-CRP12-2013-04). The authors would like to thank S. Alam at the University of Southampton for the custom built TDFA.

REFERENCES

[1] Reed, G. T. et al., "Recent breakthroughs in carrier depletion based silicon optical modulators," *Nanophotonics* 3(4-5), 229-245 (2014).
[2] Tang, Y., Peters, J. D., and Bowers, J. E., "Over 67 GHz bandwidth hybrid silicon electroabsorption modulator with asymmetric segmented electrode for 1.3 μm transmission," *Opt Express* 20(10), 11529-11535 (2012).
[3] Feng, D. et al., "High speed GeSi electro-absorption modulator at 1550 nm wavelength on SOI waveguide," *Opt Express* 20(20), 22224-22232 (2012).
[4] Liu, M. et al., "A graphene-based broadband optical modulator," *Nature* 474(64 (2011).
[5] Koos, C. et al., "Terabit/s optical transmission using chip-scale frequency comb sources," *2014 The European Conference on Optical Communication (ECOC)* 1-3 (2014).
[6] Vivien, L. et al., "Zero-bias 40Gbit/s germanium waveguide photodetector on silicon," *Opt. Express* 20(2), 1096-1101 (2012).
[7] Feng, N.-N. et al., "Vertical p-i-n germanium photodetector with high external responsivity integrated with large core Si waveguides," *Opt. Express* 18(1), 96-101 (2010).
[8] Littlejohns, C. G. et al., "50 Gb/s silicon photonics receiver with low insertion loss," *IEEE Photonics Technology Letters* 26(7), 714-717 (2014).
[9] Littlejohns, C. G. et al., "Ge-on-Si plasma enhanced chemical vapor deposition for low cost photodetectors," *IEEE Photonics Journal* 7(4), 6802408 (2015).
[10] Nedeljkovic, M. et al., "Mid-infrared thermo-optic modulators in SoI," *IEEE Photonics Technology Letters* 26(13), 1352-1355 (2014).
[11] Nedeljkovic, M. et al., "Grating coupled low loss Ge-on-Si waveguides and multimode interferometers for the mid-infrared," *Optical Fibre Communications* (2015).
[12] Mashanovich, G. Z. et al., "Silicon Photonic Waveguides and Devices for Near- and Mid-IR Applications," *Selected Topics in Quantum Electronics, IEEE Journal of* 21(4), (2015).
[13] Rouifed, M. S. et al., "Towards MZI modulator in GeOI and SOI waveguide platforms for Mid-InfraRed wavelengths," *Photonics Conference (IPC), 2015* 345-346 (2015).
[14] Rouifed, M. S. et al., "Ultra-compact MMI-based beam splitter demultiplexer for the NIR/MIR wavelengths of 1.55 μm and 2 μm," *Opt Express* 25(10), 10893-10900 (2017).
[15] Rouifed, M. S. et al., "Low Loss SOI Waveguides and MMIs at the MIR Wavelength of 2 μm," *IEEE Photonics Technology Letters* 28(24), 2827-2829 (2016).
[16] Li, Z. et al., "Diode-pumped wideband thulium-doped fiber amplifiers for optical communications in the 1800 – 2050 nm window," *Opt Express* 21(22), 26450-26455 (2013).
[17] Poletti, F. et al., "Towards high-capacity fibre-optic communications at the speed of light in vacuum," *Nature Photonics* 7(279 (2013).
[18] Petrovich, M. N. et al., "Demonstration of amplified data transmission at 2 μm in a low-loss wide bandwidth hollow core photonic bandgap fiber," *Opt Express* 21(23), 28559-28569 (2013).
[19] Nedeljkovic, M., Soref, R., and Mashanovich, G. Z., "Free-Carrier Electrorefraction and Electroabsorption Modulation Predictions for Silicon Over the 1-14 μm Infrared Wavelength Range," *IEEE Photonics Journal* 3(6), 1171-1180 (2011).
[20] Ackert, J. J. et al., "High-speed detection at two micrometres with monolithic silicon photodiodes," *Nat Photon* 9(6), 393-396 (2015).